

Broad- and narrow-line terahertz filtering in frequency-selective surfaces patterned on thin low-loss polymer substrates

Antonio Ferraro, Dimitrios C. Zografopoulos, Roberto Caputo, and Romeo Beccherelli

Abstract—A new class of frequency-selective surface filters (FSS) for terahertz (THz) applications is proposed and investigated both numerically and experimentally. A periodic FSS array of cross-shaped apertures is patterned on aluminum, deposited on thin foils of the low-loss cyclo-olefin polymer Zeonor. Apart from the fundamental filtering response of the FSS elements, we also observe very narrow-linewidth peaks with high transmittance, associated with guided-mode resonances in the dielectric substrate. The effect of the filter’s geometrical parameters on its performance is systematically studied via finite-element simulation and confirmed by time-domain spectroscopy characterization of the fabricated samples. Finally, thanks to the flexibility of the employed substrates, THz-FSS filters are also characterized in bent configuration, revealing a robust response in terms of the fundamental FSS passband filter and a high sensitivity of the GMR peaks. These features can be exploited in the design of novel THz filters or sensors.

Index Terms—Terahertz photonics, frequency-selective surfaces, terahertz filters, grating mode resonances, flexible devices.

I. INTRODUCTION

THE terahertz (THz) frequency range has been under intense investigation due to its numerous applications from fundamental to applied science, among which secure short-range communications, life-science diagnostics, defense and security [1]–[5]. Furthermore, this technological interest towards THz science is constantly growing, driven by recent advances in the development of novel and relatively low-cost THz sources with improved performance. In this context, the design of new components capable of manipulating the amplitude, phase, or polarization, of THz radiation is of paramount importance, and several research groups have been working on the development of such components, e.g. polarizers [6], phase shifters [7], [8], electromagnetic absorbers [9], [10], or tunable filters [11], [12].

This work was funded by the Italian Ministry of Foreign Affairs, Directorate General for the Country Promotion and by the Italian Ministry of Education, University and Research (Progetto Premiale THEIA). The authors would also like to acknowledge the contribution of the COST Action IC1208 (www.ic1208.com). They kindly thank Riccardo Musci from ZEON Co. for valuable support and the supply of materials.

A. Ferraro is with the Consiglio Nazionale delle Ricerche, Istituto per la Microelettronica e Microsistemi (CNR-IMM), Roma 00133, Italy and the Department of Physics, University of Calabria, I-87036 Rende (CS), Italy. (e-mail: antonio.ferraro@artov.imm.cnr.it)

D. C. Zografopoulos and R. Beccherelli are with the Consiglio Nazionale delle Ricerche, Istituto per la Microelettronica e Microsistemi (CNR-IMM), Roma 00133, Italy.

R. Caputo is with the Department of Physics, University of Calabria, I-87036 Rende (CS), Italy.

Photoconductive antennas and non-linear organic or inorganic crystals illuminated by fs laser pulses represent perhaps the most widely used THz sources [13], typically employed in terahertz time domain spectroscopy (THz-TDS) setups. However, their radiation is broadband, spanning a range of a few THz. In view of that, selective filters that allow for the bandpass transmission around a specific frequency are well needed. Such filters can be used also in other fields, for instance astronomy, telecommunications, imaging, detection, or radar science [14], [15], and have long attracted the attention of many researchers. The most common typology of bandpass filters in the THz frequency range is based on resonant frequency selective surfaces (FSS), already known since 1983 [16], where a polarization-independent square periodic array of cross-shaped apertures was patterned on a free-standing nickel foil. Later, Porterfield *et al.* [17] applied the same geometry using copper; these two seminal works established the main design rules and explain how the performance of the filters depends on their geometry.

Nevertheless, free-standing FSS filters or, in general, THz components are fragile and need a mechanical support [18]–[20], which raises their cost and may render both their fabrication and use problematic. To alleviate this problem, various attempts have been done to fabricate FSS on dielectric substrates. The choice of the substrate material is critical as it has to be very low-loss at THz frequencies so as not to compromise the filter’s transmittance. One approach is the patterning of the FSS or any metasurface, on a few micron-thick polyimide films, either via photolithography [21], [22] or other techniques, such as the more time and cost-consuming UV-laser direct writing [23], [24]. This results in membrane-like flexible samples, which still need some kind of mechanical support. The use of thick substrates introduces rigidity but this may come at the expense of higher losses and hence lower transmittance, as in FSS filters fabricated on 1-mm thick high-density polyethylene substrates [25], [26]. In [27] a FSS filter patterned on both sides of a costly 525- μm high-resistivity silicon substrate, which presents very good out-of-band rejection, although still accompanied by moderate peak transmittance. Other substrate solutions include the use of 100- μm polyethylene terephthalate [28], [29] or naphthalate [30], which were employed in a different context, namely the design and fabrication of multi-layer stacks of split-ring resonator FSS and metamaterials in the THz spectrum [31]–[34].

In this work, we present a numerical and experimental study of aluminum-based, cross-shaped aperture FSS filters

fabricated on thin substrates made of Zeonor, a low-cost cycloolefin polymer that shows very low losses at THz frequencies. Apart from the well-known broad-line filtering response that stems from the metallic mesh FSS, we observe a series of Fano-like asymmetric narrow-line transmission peaks at higher frequencies, inside the diffraction regime.

It is well known that when the operating wavelength is smaller than the FSS lattice pitch part of the THz radiation is diffracted, which may lead to various interesting phenomena, such as diffractive coupling between adjacent FSS elements [35]–[37]. However, in the case of the here investigated metallic THz filters, we observe guided-mode resonances (GMR) that occur at resonant frequencies where the first-order diffracted waves are phased-matched and thus coupled to modes guided in the dielectric substrate. These GMR are responsible for the narrow-line peaks and their influence on the filter’s performance is thoroughly investigated.

The experimental observation of GMR at THz frequencies has been only very recently reported [38] at the frequency of approximately 7 THz. Although demonstrating the proof-of-principle, these observed GMR peaks exhibited low transmittance and broad lines owing to the use of a lossy substrate. Theoretically, it has been proposed that GMR can lead to very narrow-linewidth resonances that manifest in the spectral response of THz metamaterials [39]. In this work, we have experimentally measured THz resonances with transmittance well above 50% and full-width half-maximum (FWHM) even below 1% of the resonant frequency.

The FSS filters are fabricated using standard lithography processes, which can be scaled up to mass production using low-cost large area electronics and roll-to-roll processes. Very good agreement is observed between experimental THz-TDS measurements and finite-element numerical simulations. The resulting samples are both mechanically stable and conformable. The latter property allowed for the characterization of the filters in a bent configuration, which revealed two distinct behaviors, the robustness of the fundamental FSS filter response and the suppression of the GMR peaks. Finally, a discussion on possible applications of this novel class of FSS-THz filters in low-cost and flexible THz devices is provided.

II. NUMERICAL ANALYSIS

The schematic layout of the proposed THz-FSS filters is shown in Fig. 1. The periodic metallic FSS square lattice is characterized by the pitch P and the cross-shaped apertures are defined by the cross-arm length W and width w . The metallic screen is made of aluminum and it is supported by a thin foil of the cyclo-olefin polymer Zeonor of thickness d . The Al film thickness is 200 nm, which is thicker than the Al skin depth in the investigated frequency range, namely 150 and 58 nm at 0.3 and 2 THz, respectively. At the same time, it is thin enough in order to avoid unnecessary stressing of the polymer during the fabrication process. The thickness of the Zeonor layer is in principle an independent variable, however in this study we focus on three values, $d = 40, 100, \text{ and } 188 \mu\text{m}$, which correspond to available films for fabrication, as it will be discussed in Section III.

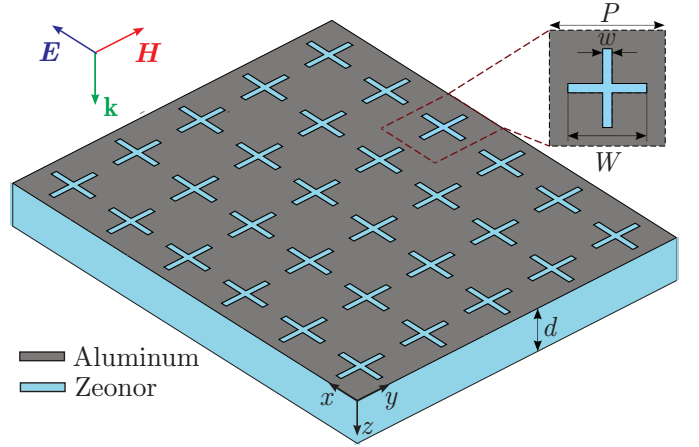


Fig. 1. Schematic layout of the investigated FSS terahertz filters. The square lattice has a pitch P and the length and width of the cross-shaped apertures are W and w , respectively. The FSS structure is patterned on a 200-nm-thick aluminum layer deposited on a Zeonor foil of subwavelength thickness d .

The numerical simulations of the THz filters was conducted via the frequency-domain finite element method (FEM), which was implemented in the commercial software COMSOL Multiphysics[®]. A unit cell of the periodic array was simulated by properly imposing periodic boundary conditions at the $x - z$ and $y - z$ planes. The structure was excited with an x -polarized plane wave propagating along the z -axis as in Fig. 1. The transmittance of the zero-order diffracted mode, i.e. the excited planewave, was measured at the exit of the filter, below the polymer film substrate, and normalized to the power carried by the excitation planewave. Aluminum was modeled as a Drude medium [40] and Zeonor as a dielectric with a refractive index equal to $n_z = 1.52 - j0.001$, as it has been demonstrated that it exhibits very low dispersion in the frequency range under investigation [41]–[43]. This polymeric material was selected for its excellent THz properties, namely very low-losses, high mechanical flexibility, heat resistance, and negligible birefringence. In fact, it was observed via numerical simulations that, in the context of the proposed THz-FSS filters and for the substrate thicknesses here reported, the effect of Zeonor’s dielectric losses was negligible.

Figure 2(a) provides a reference result on the transmittance of a free-standing THz filter, i.e. in the absence of the polymer substrate, for $P = 160 \mu\text{m}$, $W = 110 \mu\text{m}$, and $w = 10 \mu\text{m}$. A Lorentzian-shaped filter is observed with peak transmittance $T = 0.88$, resonant frequency $f_0 = 1.293 \text{ THz}$, and a FWHM of 200 GHz, i.e. $\sim 15\%$ of f_0 . The filtering effect stems from the response of THz wave transmission through the cross-shaped apertures owing to the resonance of the fundamental mode in the cross arm slots, which is maximized at the frequency f_0 , due to impedance matching [44]. When $w/(P - W) < 1$, the resonant frequency can be well approximated by the formula for resonant dipoles $f_0 = c_0/(2.1W)$ [16], marked as a dashed line in Fig. 2 and thereafter. As in other similar filters reported in the literature, this resonance only marginally depends on the pitch P , since it is not diffractive in nature, and in this work we denote it as FSS resonance (FSSR). At the frequency $f_2 = c_0/P$ that

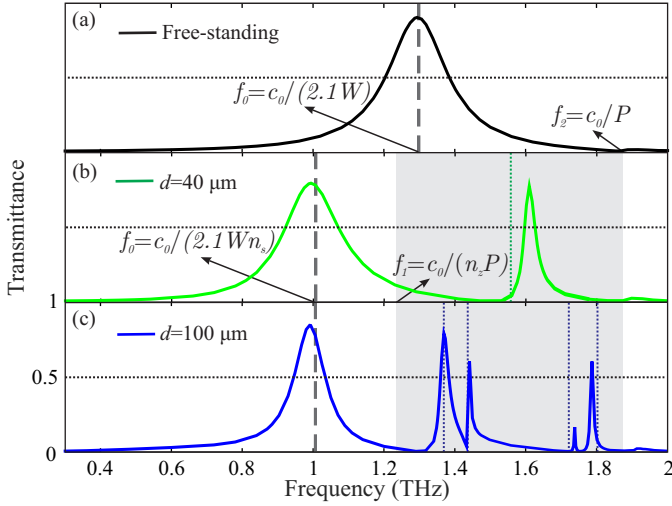


Fig. 2. (a) Power transmittance of the zero-order diffracted mode, numerically calculated for a free-standing FSS filter with $P = 160 \mu\text{m}$, $W = 110 \mu\text{m}$, and $w = 10 \mu\text{m}$. The dashed line corresponds to the frequency f_0 predicted by the approximative formula for resonant dipoles, whereas f_2 denotes the onset of the first diffractive order, associated with Wood's anomaly that leads to zero transmittance at the frequency f_2 . (b,c) Transmittance of the filter for a substrate thickness $d = 40 \mu\text{m}$ and $d = 100 \mu\text{m}$, respectively, where other parameters as in (a). The shaded region denotes the frequency interval where guided-mode resonance can manifest and the dotted lines mark the resonant frequencies predicted by GMR theory.

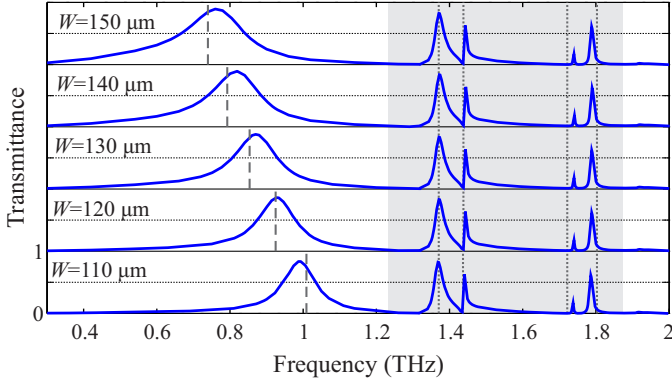


Fig. 3. Transmittance of the FSS filter for $d = 100 \mu\text{m}$, $P = 160 \mu\text{m}$, $w = 10 \mu\text{m}$, for various values of the cross-arm length W . The main resonant frequency f_0 shifts towards lower frequencies for higher W , whereas the GMRs remain unaffected. The spectral position of the GMRs is well approximated by calculating the frequencies $f_i = c_0 / (n_{\text{eff},i} P)$, marked as dashed lines, where n_i are the effective indices of the modes supported by the single Zeonor slab waveguide.

marks the threshold at which the first diffractive order appears, c_0 being the speed of light in free-space, the Wood's anomaly associated with zero transmittance is observed [21], [45].

Figures 2(b) and 2(c) investigate the same FSS structure, albeit in the presence of the Zeonor substrate, with a thickness of 40 and 100 μm , respectively. Compared to the free-standing reference case of Fig. 2(a), two major differences are observed. First, the FSSR is shifted towards lower frequencies by a factor

$$n_s = \sqrt{\frac{(n_{zr}^2 + 1)}{2}}, \quad (1)$$

where n_{zr} is the real part of n_z , and n_s is the index corresponding to the average permittivity of materials on the

TABLE I
SIMULATED GUIDED-MODE RESONANT FREQUENCIES (IN THZ) FOR THE FILTERS STUDIED IN FIG. 3.

W (μm)	$f_r^{1,\text{sim}}$	$f_r^{2,\text{sim}}$	$f_r^{3,\text{sim}}$	$f_r^{4,\text{sim}}$
150	1.371	1.443	1.743	1.797
140	1.372	1.445	1.749	1.803
130	1.373	1.448	1.753	1.809
120	1.375	1.451	1.753	1.815
110	1.379	1.453	1.753	1.817

The resonances predicted via GMR theory (dashed lines) occur at $f_r^1 = 1.37 \text{ THz}$, $f_r^2 = 1.438 \text{ THz}$, $f_r^3 = 1.733 \text{ THz}$, and $f_r^4 = 1.803 \text{ THz}$, and the corresponding slab modal indices [48] are $n_1 = 1.368$, $n_2 = 1.302$, $n_3 = 1.081$, and $n_4 = 1.038$.

two sides of the FSS, namely air and Zeonor. Equation (1) is valid for substrate thicknesses higher than one tenth of the THz wavelength [21], which is the case for the considered values of d . In general, in the presence of a substrate or superstratum the THz wave has a shorter wavelength in the dielectric medium, the cross dimensions become electromagnetically larger and the FSSR frequency decreases. Second, apart from the FSSR, other resonances are observed, whose number and position depends on the polymer thickness. These resonances stem from the coupling of waves diffracted on the periodic FSS screen to propagating modes in the substrate, which can be thought of as a dielectric slab waveguide, a phenomenon known as GMR. Grating filters based in GMR have been long known in the field of optics and photonics [46] and recently it has been shown that bandpass GMR filters can also be designed at THz frequencies, where the role of the anti-reflecting surface [47] can be played by the metallic FSS layer [38].

According to GMR theory, first-order resonances for normal incidence can be observed in the interval

$$\frac{c_0}{n_{zr} P} \leq f_r \leq \frac{c_0}{P}, \quad (2)$$

at those resonant frequencies f_r that satisfy $n_i = c_0 / (f_r P)$, where n_i is the effective index of a mode guided in the substrate slab waveguide. In Figs. 2(b) and 2(c) we have annotated with grey shading the spectral window where GMR can occur. Inside these regions, we have calculated a set of GMR frequencies, marked as dotted lines, according to the following steps: first, the resonant frequencies f_r calculated by the FEM simulations are identified, i.e. the transmission maxima in the gray-shaded areas of the calculated spectra. Then, for each slab thickness the effective modal indices at f_r are calculated using a freely available electromagnetic mode solver for 1-D dielectric multilayer slab waveguides [48]. Among the resulting modal indices $n_i(f_r)$, the frequencies $c_0 / (n_i P)$ are calculated and the one closely matching f_r is marked, with each resonant frequency associated with a different slab mode. Better agreement is achieved for higher values of d and for modes closer to the limit $f_1 = c_0 / (n_{zr} P)$. In both cases, these modes show higher confinement thanks to either the higher slab thickness or the higher effective modal index and hence lower modal order. The discrepancy between GMR theory and FEM simulations is attributed to the presence of the reflecting metallic FSS screen, which introduces a perturbation in the geometry of the slab waveguide.

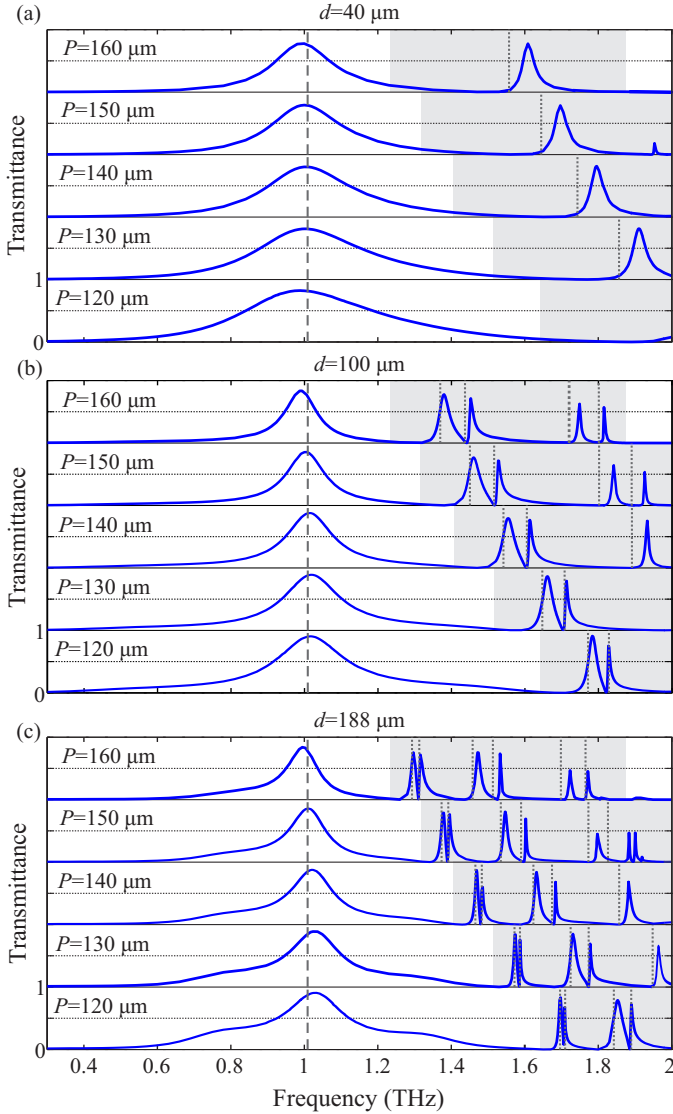


Fig. 4. Transmittance of the FSS filter numerically calculated for $W = 110 \mu\text{m}$, $w = 10 \mu\text{m}$, various values of the lattice pitch P and for three commercially available thicknesses of the Zeonor substrate, namely (a) $d = 40 \mu\text{m}$, (b) $d = 100 \mu\text{m}$, and (c) $d = 188 \mu\text{m}$. The main resonant frequency f_0 remains fixed at $f_0 \simeq c_0/(2.1Pn_s)$, whereas the GMRs shift as a function of the lattice pitch and the substrate thickness.

It is clear that the positions of the GMR frequencies depend strongly on d and P , as these parameters control the matching condition between the wave vector of the diffracted orders and the propagating substrate modes. This strong dependence is not to be expected as far as the exact geometry of the cross-shaped apertures is concerned. In order to further elucidate this point, we have calculated the transmittance of a series of filters with fixed $d = 100 \mu\text{m}$, $P = 160 \mu\text{m}$, $w = 10 \mu\text{m}$, for various values of the cross-arm length W . The results reported in Fig. 3 demonstrate that the GMR are only slightly affected by the variation of W , as summarized in the results of Table I, while the opposite stands for the FSSR, which depends on W via $f_0 = c_0/(2.1Wn_s)$. Figure 4 investigates a complementary scenario, namely the variation of the pitch P for an FSS with fixed $W = 110 \mu\text{m}$, $w = 10 \mu\text{m}$, for

the three available thicknesses of the Zeonor film thickness. In this case it is the FSS resonant frequency f_0 that remains approximately at the same position, while those of the GMR shift towards lower frequencies for higher pitch values, given the condition described by Eq. (2). Moreover, as d gets higher, a larger number of GMR is supported that corresponds to a higher number of modes guided in the slab waveguide, whose positions are well resolved by the numerical simulations described above.

Apart from the interesting underlying physics, the GMR filters show also great potential in view of THz applications that need narrow-line selective filtering. In this respect, one main drawback of the traditional FSSR filters is that their linewidth, defined as FWHM/f_0 , is in the range 5% \sim 20%, according to the various designs [38]. Achieving more narrow filters is possible by reducing the aperture's dimensions, particularly w , or by stacking more than one FSS filters, although this comes to the expense of significantly reduced transmittance. On the contrary GMR-based THz filters can have linewidths lower than 1% [38], without compromising the filter's transmittance, which is validated both numerically and experimentally in this work.

III. EXPERIMENTAL DEMONSTRATION

We have experimentally investigated the properties of the proposed THz filters by fabricating samples with different period and cross-arm length values on low-loss flexible 40, 100, and 188- μm -thick Zeonor[®] foils using standard photolithography techniques. First, an aluminum layer of 200 nm thickness was thermally evaporated on Zeonor foils. Subsequently, a film of the positive photoresist S1813 from Shipley was deposited by spin-coating at 3000 rpm for 30 seconds and then cured at 115°C for 2 minutes. The resulting thickness of the photoresist layer was $1.3 \pm 0.1 \mu\text{m}$. Photolithography was carried out on the metalized surface using a Karl Suss MA150 mask aligner with a wavelength of 365 nm and intensity of 60 mW/cm². The samples were immersed in the developer MF319 for 50 seconds, rinsed with deionized water, dried with nitrogen and cured at 120°C for 5 minutes. Then, the exposed aluminum was wet-etched in $\text{H}_3\text{PO}_4:\text{H}_2\text{O}:\text{CH}_3\text{COOH}:\text{HNO}_3=16:2:1:1$ and the residual photoresist was removed with acetone. The filters were cut in samples of 2 cm \times 2 cm.

The transmission properties of the fabricated THz filters were investigated by means of THz time domain spectroscopy using a Menlo Systems TERA K15 THz-TDS all fiber-coupled spectrometer in transmission mode using collimated and polarized radiation. The power transmittance measured for each sample was normalized to that of the reference signal, i.e. in the absence of the sample. The spot-size of the collimated beam was approximately 10 mm in diameter and a time scan of 400 ps was employed for a spectral resolution of 2.5 GHz. The measurements were done in an atmosphere purged with nitrogen to prevent the absorption of THz radiation from water vapor in the air.

Figure 5 shows a direct comparison between the numerically simulated transmittance of the THz filters, calculated by means of the finite-element method, and the experimental

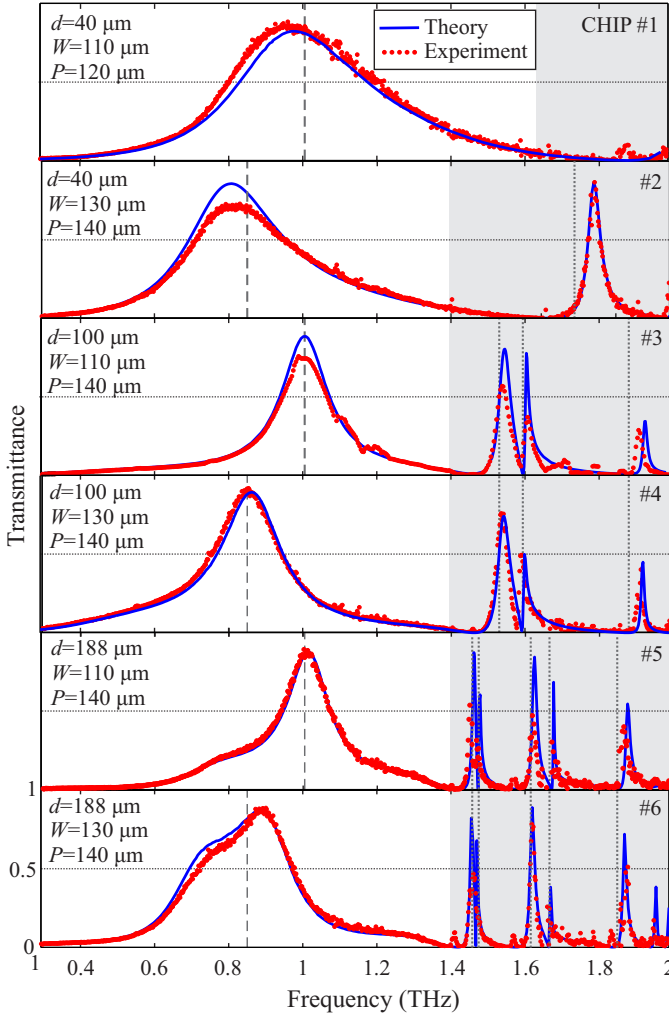


Fig. 5. Direct comparison of the FSS filter's transmittance between numerical FEM simulations and experimental TDS measurements for a series of fabricated samples with different geometrical parameters.

TDS measurements for six different chips, two for each one of the available Zeonor foil substrates. The experimental results reproduce very well the numerical simulations, in terms of both the position and the lineshape of the various transmission peaks. For $d = 40 \mu\text{m}$ and $P = 140 \mu\text{m}$ (Chip #2) two clearly separated resonances are observed, the FSSR at 0.8 THz and a single GMR at 1.8 THz. It is experimentally verified that, owing to the different underlying physical mechanisms, these two resonances show very different linewidths: the FWHM measured for the FSSR and GMR is 40% and only 2.3% of the resonant frequency, respectively. For $d = 100 \mu\text{m}$ and $188 \mu\text{m}$, the existence of closely spaced GMR peaks, stemming from the excitation of more modes in the slab waveguide substrate, leads to asymmetric Fano-like linewidths [49], with high transmittance and even more narrow linewidths. For instance, Chip #4 is characterized by three GMR at 1.546, 1.597, 1.921 THz with linewidths FWHM/f_0 equal to 2.5%, 1.3%, and 1%, respectively, while the high-transmittance resonances at 1.63 and 1.88 THz for Chip #6 exhibit corresponding linewidths of 1% and 0.7%.

It is observed that in the case of some GMR the experimen-

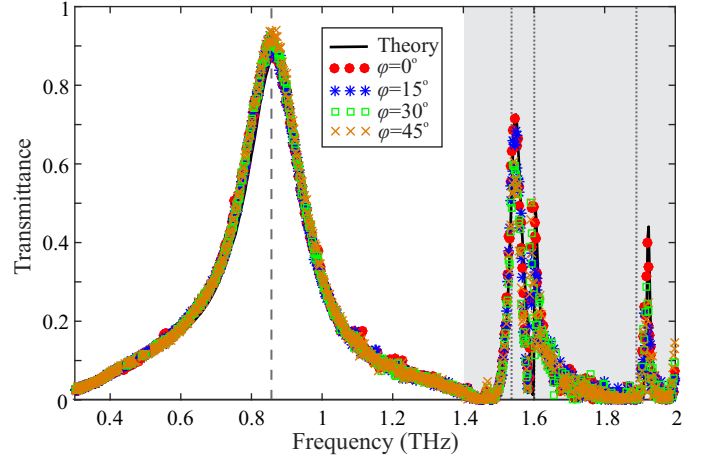


Fig. 6. TDS measurements of Chip #4, as in Fig. 5, for different angles φ of the sample's rotation in the $x-y$ plane, demonstrating polarization-insensitive operation.

tally measured transmittance peak values are somewhat lower than the numerically calculated prediction. This is attributed to three factors: a) the very narrow linewidths of such resonances, particularly for $d = 188 \mu\text{m}$, which are comparable with the TDS resolution, b) minor defects in fabrication or the planarity of the samples, c) non-ideal collimation/ residual divergence of the spot, and d) the finite dimensions of the sample and THz spot, with a diameter of a few tens of wavelength in size, in contrast to the infinite periodic array assumed in the simulations. The latter, in particular, is very relevant for GMR, since these are numerically simulated as the result of constructive interference of the excited waveguide modes and the diffractive waves on an infinite periodic FSS metallic screen, while the measurements are conducted over a finite truncated lattice. Nevertheless, apart from these small discrepancies, it is overall demonstrated that the fabricated FSS-THz filter can achieve both broad- and narrow-band filtering, depending on the selection of the geometrical parameters.

An important trait of the proposed THz filters is that they are polarization-independent, owing to the square FSS lattice and the symmetry of the cross-shaped apertures. This has been experimentally verified by rotating the fabricated samples in the $x-y$ plane, i.e. perpendicular to the propagation direction of the x -polarized THz wave, and recording the measured TDS spectra. Figure 6 shows a set of results obtained for the filter characterized by $P = 140 \mu\text{m}$, $W = 110 \mu\text{m}$, $w = 10 \mu\text{m}$, and $d = 100 \mu\text{m}$ (Chip #4 with reference to Fig. 5), where the angle φ denotes the rotation angle of the sample, measured from the x -axis. The spectra recorded for $\varphi = 0^\circ$, 15° , 30° , and 45° overlap, thus demonstrating the polarization-independent response of the THz filter.

Among the appealing properties of the employed thin polymer films are their flexibility and ability to easily conform to curved surfaces [6]. In this work, we have experimentally investigated the transmission properties of Chip #4, when bent down to a curvature with radius 1 cm. The inset of Fig. 7(a) shows a micrograph of the fabricated filter taken under optical microscope in transmission mode with a 20x

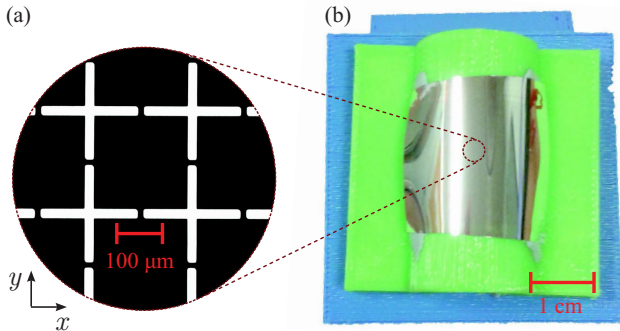


Fig. 7. (a) Micrograph taken under the microscope in transmission mode of a fabricated sample with $P = 140 \mu\text{m}$, $W = 130 \mu\text{m}$, and $w = 10 \mu\text{m}$ on a Zeonor foil with $d = 100 \mu\text{m}$. (b) The same sample bent at a radius of 1 cm and fixed on a properly assembled mount in order to characterize its properties as a conformal THz filter.

microscope objective, where the black parts are aluminum, while the transparent foil appears white. Figure 7(b) shows the bent sample mounted on a properly designed frame, so that it is placed in the THz beam path of the TDS setup. It is remarked that, after processing, the filter does not show any buckling and maintains its mechanical and electromagnetic properties after bending it several times.

Figure 8 shows the experimental characterization of the bent THz filter, where the numerical and experimental results for the flat configuration are also reported for comparison. In the experimental characterization, the incoming THz wave was polarized along the x -axis, as defined in Fig. 7. It is evident that the bent filter retains its filtering property as far as the FSSR is concerned, while all remaining peaks that stem from GMR excitation are no longer observed. These interesting features can be explained by taking into account the physical origin of the filter's resonances. The FSSR involves the excitation of a localized mode inside the cross-shaped aperture, which depends on the aperture's dimensions and is not diffractive in nature, hence the very weak dependence of its central frequency on the lattice pitch, as demonstrated in Fig. 4. Also, the presence of the substrate induces a shift of the resonant frequency by the factor n_s , but does not otherwise affect the transmission mechanism of the filter.

On the contrary, the GMR are excited due to the coupling of first-order diffracted waves into the substrate slab modes. This coupling is strongly dependent on both the lattice pitch and the polymer film's thickness. When the sample is bent, the impinging THz plane wave does not sample the same effective pitch across the filter's surface and the substrate is no longer a flat slab dielectric waveguide. This leads to the suppression of GMR peaks, as evidenced in the results of Fig. 8. Therefore, apart from the filtering properties already demonstrated in Fig. 5 for the flat configuration, the proposed THz filters show very interesting properties also when bent, which can be readily exploited in various applications. For instance, flexible filters based on the FSSR can be designed for use as thin conformal layers on curved surfaces or components in THz setups. Moreover, the sensitivity of the GMR transmittance and central frequencies on the bending radius can provide

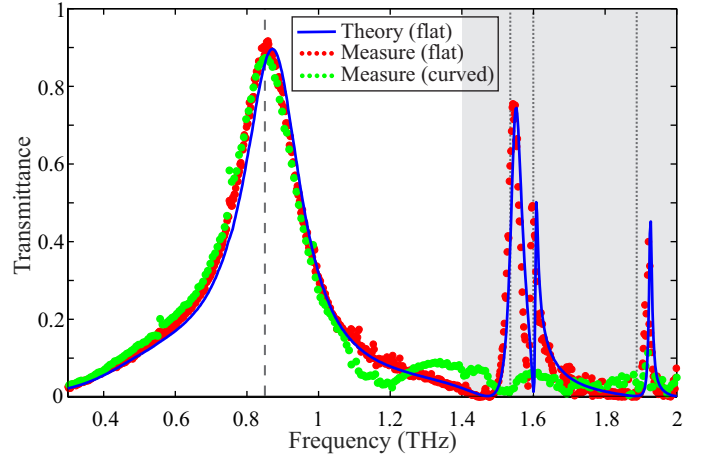


Fig. 8. Comparison of the experimentally measured transmittance of the FSS filter shown in Fig. 7 between the flat and bent configuration. The numerical simulations for the flat case are also shown for reference. The main FSS resonance remains unaffected, demonstrating the capability of the fabricated samples to operate as flexible and conformal thin film THz filters. The GMR peaks in the bent configuration are suppressed.

the basis for the development of sensor devices, for instance curvature sensors or components for the measurement of the thickness and/or refractive index of thin dielectric layers at THz frequencies by placing the FSS-GMR filters on top of the sample and measuring the shift of the GMR frequencies.

IV. CONCLUSIONS

In brief, we have numerically and experimentally investigated a new class of THz filters based on the patterning of metallic cross-shaped FSS on thin films of the low-loss cycloolefin polymer Zeonor. By properly adjusting the geometrical parameters of the device both broad- and narrowline filters can be designed, the first stemming from the transmittance of THz waves through FSS cross-shaped apertures, while the latter from the excitation of guided-mode resonances in the polymer substrate. Not observed before in this kind of FSS structures, the GMR filters show extremely narrow linewidths with high transmittance. The FSS filters are shown robust to the bending of the flexible Zeonor films, thus paving the way for conformal THz filters integrated on curved surfaces. On the contrary, the diffractive nature of GMR renders them sensitive to deformations or changes of the substrate's properties, properties that could be exploited in the design of sensors working at THz frequencies.

REFERENCES

- [1] X. C. Zhang and J. Xu, *Introduction to THz Wave Photonics*, Springer, Oregon, USA, 2010.
- [2] I. F. Akyildiz, J. M. Jornet, and C. Han, "Terahertz band: Next frontier for wireless communications," *Phys. Commun.*, vol. 12, pp. 16–32, 2014.
- [3] K. R. Jha and G. Singh, *Terahertz Planar Antennas for Next Generation Communication*, Springer, 2014.
- [4] E. P. J. Parrott, Y. Sun, and E. Pickwell-MacPherson, "Terahertz spectroscopy - Its future role in medical diagnoses," *J. Mol. Struct.*, vol. 1006, pp. 66–76, 2011.
- [5] K. E. Peiponen, J. A. Zeitler, and M. Kuwata-Gonokami, *Terahertz Spectroscopy and Imaging*, Springer, 2013.

- [6] A. Ferraro, D. C. Zografopoulos, M. Missori, M. Peccianti, R. Caputo, and R. Beccherelli, "Flexible terahertz wire grid polarizer with high extinction ratio and low loss," *Opt. Lett.*, vol. 41, pp. 2009–2012, 2016.
- [7] D. C. Zografopoulos and R. Beccherelli, "Tunable terahertz fishnet metamaterials based on thin nematic liquid crystal layers for fast switching," *Sci. Rep.*, vol. 5, art. no. 13137, 2015.
- [8] K. Altmann, M. Reuter, K. Garbat, M. Koch, R. Dąbrowski, and I. Dierking, "Polymer stabilized liquid crystal phase shifter for terahertz waves" *Opt. Express*, vol. 21, pp. 12395–12400, 2013.
- [9] K. Iwaszczuk, A. C. Strikwerda, K. Fan, X. Zhang, R. D. Averitt, and P. U. Jepsen, "Flexible metamaterial absorbers for stealth applications at terahertz frequencies," *Opt. Express*, vol. 20, pp. 635–643, 2012.
- [10] G. Isić, B. Vasić, D. C. Zografopoulos, R. Beccherelli, and R. Gajić, "Electrically tunable critically coupled terahertz metamaterial absorber based on nematic liquid crystals," *Phys. Rev. Applied*, vol. 3, art. no. 064007, 2015.
- [11] H. Němec et al., "Thermally tunable filter for terahertz range based on a one-dimensional photonic crystal with a defect," *J. Appl. Phys.*, vol. 96, pp. 4072–4075, 2004.
- [12] A. Ferraro, D. C. Zografopoulos, R. Caputo, and R. Beccherelli, "Periodical elements as low-cost building blocks for tunable terahertz filters," *IEEE Photon. Technol. Lett.*, doi:10.1109/LPT.2016.2600645, 2016.
- [13] R. A. Lewis, "A review of terahertz sources," *J. Phys. D*, vol. 47, art. no. 374001, 2014.
- [14] A. M. Melo, A. L. Gobbi, M. H. O. Piazzetta, and A. M. P. A. da Silva, "High-selectivity bandpass frequency-selective surface in terahertz band," *Adv. Opt. Technol.*, vol. 2012, art. no. 530512, 2012.
- [15] R. J. Williams, A. J. Gatesman, T. M. Goyette, and R. H. Giles, "Radar cross section measurements of frequency selective terahertz retroreflectors," *Proc. SPIE*, vol. 9102, art. no. 91020R, 2014.
- [16] S. T. Chase and R. D. Joseph, "Resonant array bandpass filters for the far infrared," *Appl. Opt.*, vol. 22, pp. 1775–1779, 1983.
- [17] D. W. Porterfield, J. L. Hesler, R. Densing, E. R. Mueller, T. W. Crowe, and R. M. Weikle, "Resonant metal-mesh bandpass filters for the far infrared," *Appl. Opt.*, vol. 33, pp. 6046–6052, 1994.
- [18] Thorlabs, Inc., "THz Bandpass Filters: 10 μm - 590 μm Center Wavelength", (https://www.thorlabs.com/newgrouppage9.cfm?objectgroup_id=7611).
- [19] Tydex, "THz Band Pass Filters", (http://www.tydexoptics.com/products/thz_optics/thz_band_pass_filter).
- [20] N. Born, R. Gente, I. Al-Naib, and M. Doskolovich, "Laser beam machined free-standing terahertz metamaterials," *Electron. Lett.*, vol. 51, pp. 1012–1014, 2015.
- [21] M. E. MacDonald, A. Alexanian, R. A. York, Z. Popović, and E. N. Grossman, "Spectral transmittance of lossy printed resonant-grid terahertz bandpass filters," *IEEE Trans. Microw. Theory Techn.*, vol. 48, pp. 712–718, 2000.
- [22] J.-H. Kim, M. P. Hokmabadi, S. Bolci, E. Rivera, D. Wilbert, P. Kung, and S. M. Kim, "Investigation of robust flexible conformal THz perfect metamaterial absorber," *Appl. Phys. A*, vol. 122, art. no. 362, 2016.
- [23] H. Tao, A. C. Strikwerda, K. Fan, C. M. Bingham, W. J. Padilla, X. Zhang, and R. D. Averitt, "Terahertz metamaterials on free-standing highly-flexible polyimide substrates," *J. Phys. D*, vol. 41, art. no. 232004, 2008.
- [24] B. Voisiat, A. Bičiūnas, I. Kašalynas, and G. Račiukaitis, "Bandpass filters for THz spectral range fabricated by laser ablation," *Appl. Phys. A*, vol. 104, pp. 953–958, 2011.
- [25] Y. Ma, A. Khalid, T. D. Drysdale, and D. R. S. Cumming, "Direct fabrication of terahertz optical devices on low-absorption polymer substrates," *Opt. Lett.*, vol. 34, pp. 1555–1557, 2009.
- [26] Y. Ma, A. Khalid, S. C. Saha, J. P. Grant, and D. R. S. Cumming, "THz band pass filter on plastic substrates and its application on biological sensing," Photonics Society Winter Topicals Meeting Series (WTM), IEEE, pp. 50–51, 2010.
- [27] A. C. Strikwerda, M. Zalkovskij, D. L. Lorenzen, A. Krabbe, A. V. Lavrinenko, and P. U. Jepsen, "Metamaterial composite bandpass filter with an ultra-broadband rejection bandwidth of up to 240 terahertz," *Appl. Phys. Lett.*, vol. 104, art. no. 191103, 2014.
- [28] F. Miyamaru, M. W. Takeda, and K. Taima, "Characterization of terahertz metamaterials fabricated on flexible plastic films: toward fabrication of bulk metamaterials in terahertz region," *Appl. Phys. Express*, vol. 2, art. no. 042001, 2009.
- [29] F. Miyamaru, S. Kuboda, K. Taima, K. Takano, M. Hangyo, and M. W. Takeda, "Three-dimensional bulk metamaterials operating in the terahertz range," *Appl. Phys. Lett.*, vol. 96, art. no. 081105, 2010.
- [30] N. R. Han, Z. C. Chen, C. S. Lim, B. Ng, and M. H. Hong, "Broadband multi-layer terahertz metamaterials fabrication and characterization on flexible substrates," *Opt. Express*, vol. 19, pp. 6990–6998, 2011.
- [31] O. Paul, R. Beigang, and M. Rahm, "Highly selective terahertz bandpass filters based on trapped mode excitation," *Opt. Express*, vol. 17, pp. 18590–18595, 2009.
- [32] L. Liang, B. Jin, J. Wu, Y. Huang, Z. Ye, X. Huang, D. Zhou, G. Wang, X. Jia, H. Lu, L. Kang, W. Xu, J. Chen, and P. Wu, "A flexible wideband bandpass terahertz filter using multi-layer metamaterials," *Appl. Phys. B*, vol. 113, pp. 285–290, 2013.
- [33] D. S. Wang, B. J. Chen, and C. H. Chan, "High-selectivity bandpass frequency-selective surface in terahertz band," *IEEE Trans. THz Sci. Technol.*, vol. 6, pp. 284–291, 2016.
- [34] Y.-J. Chiang, C.-S. Yang, Y.-H. Yang, C.-L. Pan, and T.-J. Yen, "An ultrabroad terahertz bandpass filter based on multiple-resonance excitation of a composite metamaterial," *Appl. Phys. Lett.*, vol. 99, art. no. 191909, 2011.
- [35] R. Singh, C. Rockstuhl, F. Lederer, and W. Zhang, "The impact of nearest neighbor interaction on the resonances in terahertz metamaterials," *Appl. Phys. Lett.*, vol. 94, art. no. 021116, 2009.
- [36] A. Bitzer, J. Wallauer, H. Helm, H. Merbold, T. Feurer, and M. Walther, "Lattice modes mediate radiative coupling in metamaterial arrays," *Opt. Express*, vol. 17, pp. 22108–22113, 2009.
- [37] I. Al-Naib, C. Jansen, R. Singh, M. Walther, and M. Koch, "Novel THz metamaterial designs: from near- and far-field coupling to high-Q resonances," *IEEE Terahz. Sci. Technol.*, vol. 3, pp. 772–782, 2013.
- [38] S. Song, F. Sun, Q. Chen, and Y. Zhang, "Narrow-linewidth and high-transmission terahertz bandpass filtering by metallic gratings," *IEEE Trans. THz Sci. Technol.*, vol. 5, pp. 131–136, 2015.
- [39] H. Chen, J. Liu, and Z. Hong, "Guided mode resonance with extremely high Q-factors in terahertz metamaterials," *Opt. Commun.*, vol. 282, pp. 508–512, 2017.
- [40] M. A. Ordal, R. J. Bell, R. W. Alexander, L. L. Long, and M. R. Querry, "Optical properties of fourteen metals in the infrared and far infrared: Al, Co, Cu, Au, Fe, Pb, Mo, Ni, Pd, Pt, Ag, Ti, V, and W," *Appl. Opt.*, vol. 24, 4493–4499, 1985.
- [41] P. A. George, W. Hui, F. Rana, B. G. Hawkins, A. E. Smith, and B. J. Kirby, "Microfluidic devices for terahertz spectroscopy of biomolecules," *Opt. Express*, vol. 16, pp. 1577–1582, 2008.
- [42] C. Brückner, B. Pradarutti, R. Müller, S. Riehermann, G. Notni, and A. Tünnermann, "Design and evaluation of a THz time domain imaging system using standard optical design software," *Appl. Opt.*, vol. 47, pp. 4994–5007, 2008.
- [43] A. Podzorov and G. Gallot, "Low-loss polymers for terahertz applications," *Appl. Opt.*, vol. 47, pp. 3254–3257, 2008.
- [44] F. Medina, F. Mesa, and R. Marqués, "Extraordinary transmission through arrays of electrically small holes from a circuit theory perspective," *IEEE Trans. Microw. Theory Techn.*, vol. 56, pp. 3108–3120, 2008.
- [45] J. Marae-Djouada, R. Caputo, N. Mahi, G. Lévéč, A. Akjouj, P.-M. Adam, and T. Maurer, "Angular plasmon response of gold nanoparticles arrays: approaching the Rayleigh limit," *Nanophotonics*, DOI:10.1515/nanoph-2016-0112, 2016.
- [46] P. Magnusson and S. S. Wang, "New principle for optical filters," *Appl. Phys. Lett.*, vol. 61, pp. 1022–1024, 1992.
- [47] S. Tibuleac and R. Magnusson, "Reflection and transmission guided-mode resonance filters," *J. Opt. Soc. Am. A*, vol. 14, pp. 1617–1626, 1997.
- [48] 1-D mode solver for dielectric multilayer slab waveguides, (<http://www.computational-photonics.eu/oms.html>)
- [49] D. A. Bykov and L. L. Doskolovich, "Spatiotemporal coupled-mode theory of guided-mode resonant gratings," *Opt. Express*, vol. 23, pp. 19234–19241, 2015.

Antonio Ferraro received the bachelor degree in Material Science and the master degree in Science and Engineering of Innovative and Functional Materials from the Physics Department of University of Calabria, Rende, Italy, in 2009 and 2012, respectively. He is currently a doctoral student in Physical, Chemical and Materials Sciences and Technologies in the same department and research fellow at the Institute for Microelectronics and Microsystems (IMM), Italian National Research Council, Rome, Italy. During his master thesis he was intern for six months at Philips Research Campus in Eindhoven, The Netherlands, under the supervision of Dr. Dick de Boer, where he was involved in projects on nanostructured luminescence materials.

His research interests include terahertz devices, plasmonic structures, nanostructured materials, liquid crystalline composite devices with particular focus on fabrication and characterization.

Dimitrios C. Zografopoulos was born in Thessaloniki, Greece, in 1980. He received the Diploma in Electrical and Computer Engineering and the Doctorate Degree from the Aristotle University of Thessaloniki (AUTH) in 2003 and 2009, respectively. In 2010 he was a Post-doctoral Fellow of the Research Committee of the AUTH and in 2011 a Post-doctoral Research Fellow of the Greek States Scholarship Foundation and a Visiting Research Fellow at the Department of Electronics Technology, Carlos III University of Madrid. He subsequently moved under a two-year Intra-European Marie-Curie Fellowship to the Institute for Microelectronics and Microsystems (IMM) of the Italian National Research Council (CNR), Rome, where he is currently employed as a Researcher.

His research interests include the design and analysis of photonic/plasmonic waveguides, liquid-crystal tunable metamaterials and devices, as well as components for THz wave manipulation. He is the author or co-author of more than 40 scientific papers in international journals and 2 book chapters.

Roberto Caputo obtained his M.Sc in Physics from the University of Calabria in 2000. In the same year he received a Post-graduate scholarship from INFN (National Institute for the Physics of Matter) for continuing his master thesis research. In 2002 he started his Ph.D in Physics. In 2005 he obtained a Marie Curie Post-doc Fellowship for the "Transfer of Knowledge" at Philips Research Laboratories in Eindhoven, The Netherlands under the supervision of Dr. Hugo Cornelissen. During the stay at Philips, his research work has been mainly focused on the realization of new-concept LCD backlight systems. In 2007 he obtained a two-year Marie Curie reintegration grant with a project on research and development of highly efficient organic lasing structures. In the same year, he obtained a position as Assistant Professor at University of Calabria and he actually is a member of CNR-NANOTEC and Physics Department of University of Calabria.

His scientific activity is mainly oriented to the study and realization of micro- and nano-scale structures in organic composite materials. Results of this research span from fundamental physics advances to innovative high-tech applications. Recently he spent a two-year period at the University of Technology of Troyes to perform advanced studies on Active Plasmonics. He has authored and co-authored more than 70 papers on international journals, 4 international patents and about 40 communications to scientific conferences and symposia. Moreover, he co-chairs the European COST Action IC1208 "Integrating devices and materials: a challenge for new instrumentation in ICT".

Romeo Beccherelli was born in Plovdiv (Bulgaria) in 1969. He received the Laurea degree cum laude in Electronic Engineering in 1994 and the Ph.D. in Electronic Engineering in 1998, both from University of Rome "La Sapienza" (Rome - Italy). In 1997 and 2001 he was Visiting Researcher Fellow at the Department of Physics - Division of Microelectronics and Nanoscience - Chalmers University of Technology (Gothemburg - Sweden). He served in the technical Corps of the Italian Army as a Second Lieutenant. In 1997 he joined the Department of Engineering Science - University of Oxford (Oxford - UK) as a Postdoctoral Research Assistant and in 2000 the Department of Electronic Engineering - University of Rome "La Sapienza" (Italy) as a Research Fellow. In 2001 he was appointed Researcher and in 2006 Senior Researcher at the Institute for Microelectronics and Microsystems of the National Research Council of Italy.

He is inventor of two patents and author of approximately 70 scientific papers in international journals, 80 conference proceedings papers and three book chapters. He has been Principal Investigator in research projects funded by the European Community, the European Space Agency and by the Italian Government, and co-coordinator of four bilateral projects. His initial research interests in liquid crystal display technology have evolved into sensor arrays, photonics and plasmonics based on liquid crystals, and into metamaterial and metasurface devices and systems for processing microwaves and terahertz waves. Dr Beccherelli's doctoral thesis was awarded the International Otto Lehman Prize 1999 in liquid crystal technology by the University of Karlsruhe (Germany) and the Otto Lehmann Foundation.